Scientific Research Publishing

International Journal of Astronomy and Astrophysics, 2018, 8, 386-405
http://www.scirp.org/journal/ijaa
ISSN Online: 2161-4725
ISSN Print: 2161-4717

Measurements of the Cosmological Parameters Ω_m and H_0

B. Hoeneisen

Universidad San Francisco de Quito, Quito, Ecuador
Email: bhoeneisen@usfq.edu.ec

How to cite this paper: Hoeneisen, B. (2018) Measurements of the Cosmological Parameters Ω_m and H_0. *International Journal of Astronomy and Astrophysics*, **8**, 386-405.
https://doi.org/10.4236/ijaa.2018.84027

Received: November 21, 2018
Accepted: December 26, 2018
Published: December 29, 2018

Abstract

From Baryon Acoustic Oscillation measurements with Sloan Digital Sky Survey SDSS DR14 galaxies, and the acoustic horizon angle θ_* measured by the Planck Collaboration, we obtain $\Omega_m = 0.2724 \pm 0.0047$, and $h + 0.020 \cdot \sum m_\nu = 0.7038 \pm 0.0060$, assuming flat space and a cosmological constant. We combine this result with the 2018 Planck "TT, TE, EE + lowE + lensing" analysis, and update a study of $\sum m_\nu$ with new direct measurements of σ_8, and obtain $\sum m_\nu = 0.27 \pm 0.08$ eV assuming three nearly degenerate neutrino eigenstates. Measurements are consistent with $\Omega_k = 0$, and $\Omega_{\text{de}}(a) = \Omega_\Lambda$ constant.

Keywords

Cosmological Parameters, Baryon Acoustic Oscillations, Galaxy Distributions, Cosmic Microwave Background

1. Introduction and Summary

From a study of Baryon Acoustic Oscillations (BAO) with Sloan Digital Sky Survey (SDSS) data release DR13 galaxies and the "sound horizon" angle θ_{MC} measured by the Planck Collaboration we obtained $\Omega_m = 0.281 \pm 0.003$ assuming flat space and a cosmological constant [1]. At the time, the 2016 Review of Particle Physics quoted $\Omega_m = 0.308 \pm 0.012$ [2]. The new 2018 Planck "TT, TE, EE + lowE + lensing" measurement [3] obtains $\Omega_m = 0.3153 \pm 0.0073$, while the "TT, TE, EE + lowE + lensing+BAO" measurement obtains $\Omega_m = 0.3111 \pm 0.0056$ [3]. Due to the growing tension between these measurements, we decided to repeat the BAO analysis in Reference [1], this time with SDSS DR14 galaxies.

The main difficulty with the BAO measurements is to distinguish the BAO signal from the cosmological and statistical fluctuations. The aim of the present analysis is to be very conservative by choosing large bins in redshift z to obtain a larger significance of the BAO signal than in [1]. As a result, the present analysis is based on 6 independent BAO measurements, compared to 18 in [1].

We assume flat space, *i.e.* $\Omega_k = 0$, and constant dark energy density, *i.e.* $\Omega_{\mathrm{de}}(a) = \Omega_\Lambda$, except in **Tables 6-8** that include more general cases. We assume three neutrino flavors with eigenstates with nearly the same mass, so $\sum m_\nu \approx 3m_\nu$. We adopt the notation of the Particle Data Group 2018 [4]. All uncertainties have 68% confidence.

The analysis presented in this article obtains $\Omega_m = 0.2724 \pm 0.0047$ so the tension has increased further. We present full details of all fits to the galaxy-galaxy distance histograms of the present measurement so that the reader may cross-check each step of the analysis. Calibrating the BAO standard ruler we obtain $h + 0.020 \cdot \sum m_\nu = 0.7038 \pm 0.0060$, where $H_0 \equiv 100h\ \mathrm{km \cdot s^{-1} \cdot Mpc^{-1}}$.

Combining the direct measurement $\Omega_m = 0.2724 \pm 0.0047$ with the 2018 Planck "TT, TE, EE + lowE + lensing" analysis obtains $\Omega_m = 0.2853 \pm 0.0040$ and $h = 0.6990 \pm 0.0030$, at the cost of an increase of the Planck χ^2_{P} from 12956.78 to 12968.64.

Finally, we update the measurement of $\sum m_\nu$ of Reference [5] with the data of this Planck + Ω_m combination, and two new direct measurements of σ_8, and obtain $\sum m_\nu = 0.27 \pm 0.08$ eV. This result is sensitive to the accuracy of the direct measurements of σ_8.

2. Measurement of Ω_m with BAO as an *Uncalibrated* Standard Ruler

We measure the comoving galaxy-galaxy correlation distance d_{drag}, in units of c/H_0, with galaxies in the Sloan Digital Sky Survey SDSS DR14 publicly released catalog [6] [7], with the method described in Reference [1]. Briefly, from the angle α between two galaxies as seen by the observer, and their red-shifts z_1 and z_2, we calculate their distance *d*, in units of c/H_0, assuming a reference cosmology [1]. At this "uncalibrated" stage in the analysis, the unit of distance c/H_0 is neither known nor needed. The adimensional distance d has a component d_α transverse to the line of sight, and a component d_z along the line of sight, given by Equation (3) of [1]. We fill three histograms of d according to the orientation of the galaxy pairs with respect to the line of sight, *i.e.* $d_z/d_\alpha < 1/3$, $d_\alpha/d_z < 1/3$, and remaining pairs. Fitting these histograms we obtain excesses centered at $\hat{d}_\alpha$, $\hat{d}_z$, and $\hat{d}_/$ respectively. Examples are shown in **Figure 1** and **Figure 2**. From each BAO observable $\hat{d}_\alpha$, $\hat{d}_/$, or $\hat{d}_z$ we recover d_{drag} for any given cosmology with Equations (5), (6), or (7) of Reference [1]. Requiring that d_{drag} be independent of red shift z and orientation we obtain the space curvature Ω_k, the dark energy density $\Omega_{\mathrm{de}}(a)$ as a function of the expansion parameter $a = 1/(1+z)$, and the matter density $\Omega_m = 1 - \Omega_{\mathrm{de}}(1) - \Omega_k - \Omega_r$. Full details can be found in [1].

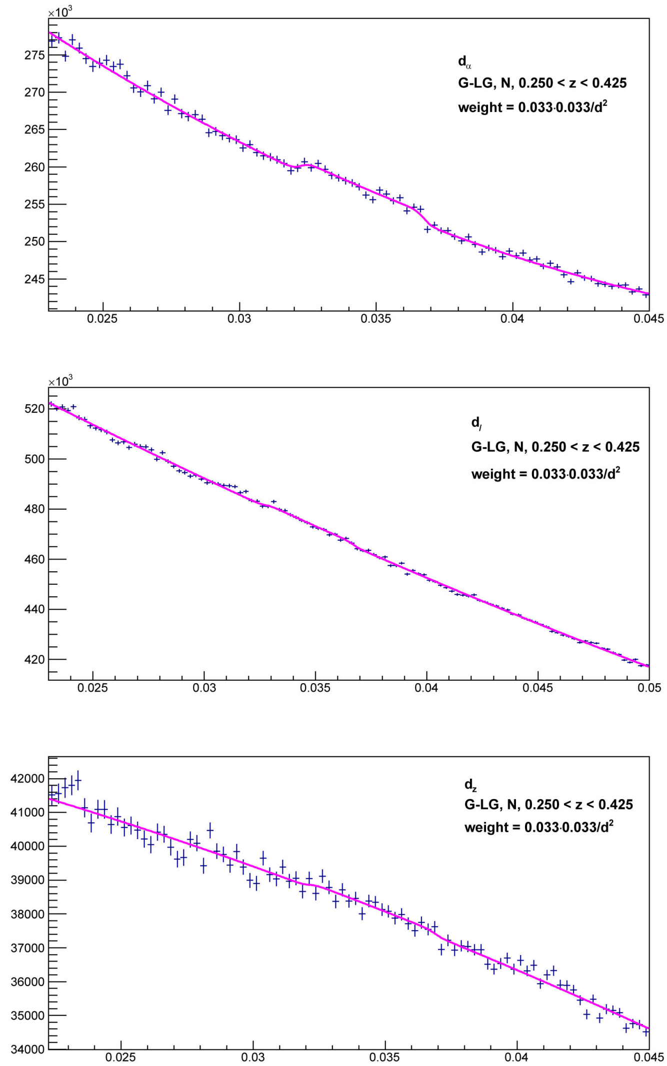

Figure 1. Fits to histograms of G-LG distances d that obtain $\hat{d}_\alpha$, $\hat{d}_/$, or $\hat{d}_z$ at $z = 0.34$. See **Table 1** and **Table 2** for details.

The challenge with these BAO measurements is to distinguish the BAO signal from the cosmological and statistical fluctuations of the background. Our strategy is three-fold: 1) redundancy of measurements with different cosmological fluctuations, 2) pattern recognition of the BAO signal, and 3) requiring all three fits for $\hat{d}_\alpha$, $\hat{d}_/$, and $\hat{d}_z$ to converge, and that the consistency relation $Q = \hat{d}_/ \big/ \left(\hat{d}_\alpha^{0.57} \hat{d}_z^{0.43}\right) = 1$ [1] be satisfied within $\pm 3\%$.

Regarding redundancy, we repeat the fits for the northern (N) and southern (S) galactic caps; we repeat the measurements for galaxy-galaxy (G-G) distances, galaxy-large galaxy (G-LG) distances, LG-LG distances, and galaxy-cluster (G-C) distances; and we fill histograms of d with weights $0.033^2/d^2$ or $0.033^2 F_i F_j / d^2$, where F_i and F_j are absolute luminosities; see [1] for details. In the present analysis we have off-set the bins of redshift z with respect to Reference [1] to obtain different background fluctuations.

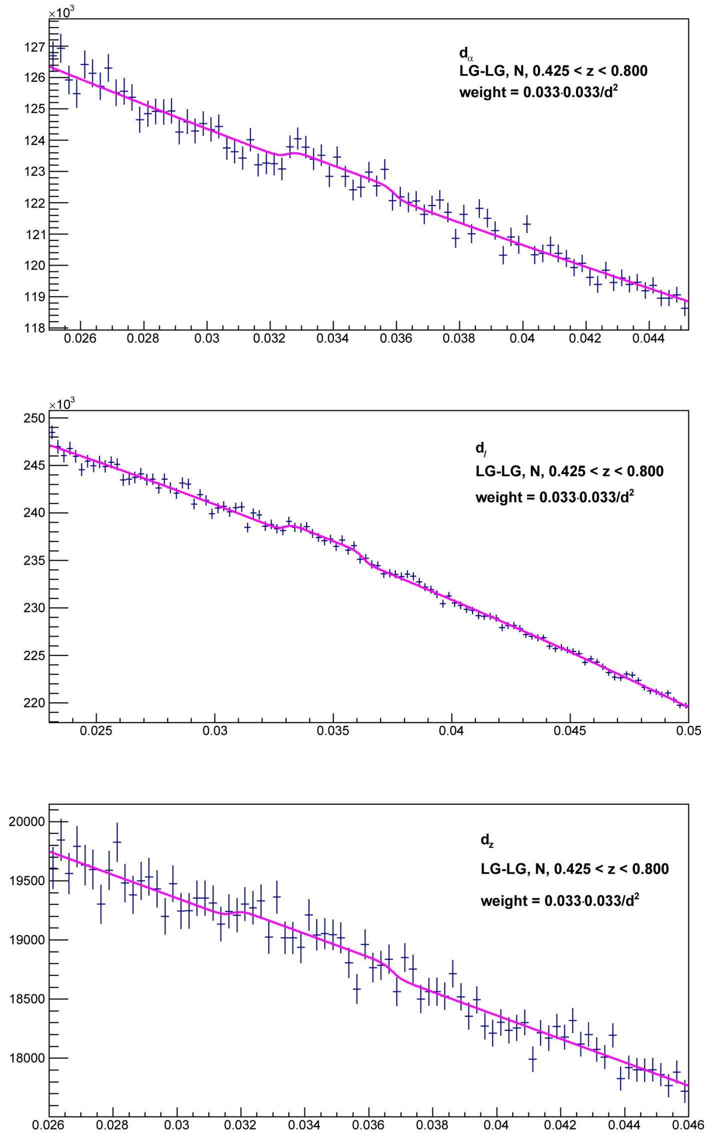

Figure 2. Fits to histograms of LG-LG distances d that obtain $\hat{d}_\alpha$, $\hat{d}_l$, or $\hat{d}_z$ at $z = 0.56$. See **Table 1** and **Table 2** for details.

Now consider pattern recognition. **Figure 1** and **Figure 2** show that the BAO signal is approximately constant from $d \approx 0.032$ to ≈ 0.037, corresponding to ≈ 137 Mpc to ≈ 158 Mpc. This characteristic shape of the BAO signal can be understood qualitatively with reference to **Figure 1** of [8]: the radial mass profile of an initial point like adiabatic excess results, well after recombination, in peaks at radii 17 Mpc and $r_{\text{drag}} \approx 148$ Mpc, so we can expect the BAO signal to extend from approximately 148-17 Mpc to 148+17 Mpc, with r_{drag} at the mid-point. From galaxy simulations described in [5], the smearing of r_{drag} due to galaxy peculiar motions has a standard deviation approximately 7.6 Mpc at $z = 0.5$, and 8.5 Mpc at $z = 0.3$. So the observed BAO signal has an unexpected "step-up-step-down" shape, and is narrower than implied by the simulation in reference [8].

The selections of galaxies are as in [1] with the added requirements for SDSS DR14 galaxies that they be "sciencePrimary" and "bossPrimary", and have a smaller redshift uncertainty zErr < 0.00025.

The fitting function has 6 free parameters, corresponding to a second degree polynomial for the background, and a "smooth step-up-step-down" function (described in [1]) with a center $\hat{d}$, a half-width Δ, and an amplitude A relative to the background. Each fit used for the final measurements is required to have a significance $A/\sigma_A > 2$ (in the analysis of [1] this requirement was $A/\sigma_A > 1$, which allows more bins of z).

Successful triplets of fits are presented in **Table 1**. Note the redundancy of measurements with $0.250 < z < 0.425$ and $0.425 < z < 800$. The independent triplets of fits selected for further analysis, are indicated with a "*", and are shown in **Figure 1** and **Figure 2**, with further details presented in **Table 2**. We note that each measurement of $\hat{d}_\alpha$, $\hat{d}_/$, or $\hat{d}_z$ in **Table 1**, together with the sound horizon angle θ_* obtained by the Planck experiment [3], is a sensitive measurement of Ω_m as shown in **Table 3**.

Table 1. Measured BAO distances $\hat{d}_\alpha$, $\hat{d}_/$, and $\hat{d}_z$, in units of c/H_0, with $z_c = 3.79$ (see [1]) from SDSS DR14 galaxies with right ascension 110˚ to 270˚, and declination −5˚ to 70˚, in the northern (N) and/or southern (S) galactic caps. Uncertainties are statistical from the fits to the BAO signal. No corrections have been applied. The independent measurements with a "*" are selected for further analysis. The corresponding fits are presented in **Figure 1** and **Figure 2**, and details are presented in **Table 2**. For comparison, measurements with a "&" correspond to SDSS DR13 data with the galaxy selections of [1].

z	z_{min}	z_{max}	Galaxies	Centers	Type	$100\hat{d}_\alpha$	$100\hat{d}_/$	$100\hat{d}_z$	Q
0.53	0.425	0.725	614,724	614,724	G-G, N+S	3.488 ± 0.015	3.504 ± 0.019	3.466 ± 0.032	1.007
0.53	0.425	0.725	614,724	13,960	G-C, N+S	3.381 ± 0.030	3.401 ± 0.033	3.395 ± 0.035	1.004
0.53	0.475	0.575	180,696	53,519	G-LG, N	3.424 ± 0.015	3.314 ± 0.018	3.242 ± 0.018	0.991
0.53	0.475	0.575	53,519	53,519	LG-LG, N	3.451 ± 0.030	3.447 ± 0.059	3.351 ± 0.022	1.012
0.53	0.475	0.575	180,696	5045	G-C, N	3.427 ± 0.031	3.331 ± 0.030	3.316 ± 0.033	0.986
0.56	0.425	0.800	230,841	230,841	G-G, S	3.441 ± 0.027	3.422 ± 0.017	3.497 ± 0.040	0.988
0.56	0.425	0.800	355,737	120,499	G-LG, N	3.425 ± 0.015	3.465 ± 0.016	3.351 ± 0.025	1.021
*0.56	0.425	0.800	120,499	120,499	LG-LG, N	3.424 ± 0.021	3.461 ± 0.018	3.424 ± 0.039	1.011
&0.56	0.425	0.800	143,778	143,778	LG-LG, N	3.424 ± 0.014	3.478 ± 0.015	3.451 ± 0.026	1.012
0.56	0.425	0.800	586,578	13,206	G-C, N+S	3.453 ± 0.038	3.365 ± 0.044	3.354 ± 0.028	0.987
0.52	0.425	0.575	236,693	236,693	G-G, N	3.437 ± 0.031	3.423 ± 0.026	3.432 ± 0.025	0.997
0.52	0.425	0.575	236,693	72,297	G-LG, N	3.416 ± 0.017	3.441 ± 0.012	3.385 ± 0.018	1.011
0.52	0.425	0.575	72,297	72,297	LG-LG, N	3.456 ± 0.033	3.447 ± 0.022	3.392 ± 0.060	1.006
0.48	0.425	0.525	151,938	4143	G-C, N	3.424 ± 0.051	3.383 ± 0.026	3.343 ± 0.062	0.998
0.36	0.250	0.450	114,597	114,597	G-G, N	3.456 ± 0.018	3.386 ± 0.015	3.318 ± 0.056	0.997
0.36	0.250	0.450	114,597	65,130	G-LG, N	3.455 ± 0.010	3.358 ± 0.015	3.293 ± 0.032	0.992
0.36	0.250	0.450	65,130	65,130	LG-LG, N	3.462 ± 0.016	3.352 ± 0.025	3.307 ± 0.039	0.988
0.34	0.250	0.425	92,321	92,321	G-G, N	3.439 ± 0.013	3.473 ± 0.015	3.423 ± 0.076	1.012
0.34	0.250	0.425	149,849	149,849	G-G, N+S	3.437 ± 0.014	3.367 ± 0.013	3.444 ± 0.042	0.979
*0.34	0.250	0.425	92,321	55,980	G-LG, N	3.449 ± 0.008	3.471 ± 0.013	3.450 ± 0.034	1.006
&0.34	0.250	0.425	133,729	94,873	G-LG, N	3.431 ± 0.011	3.469 ± 0.014	3.383 ± 0.024	1.017
0.34	0.250	0.425	55,980	55,980	LG-LG, N	3.467 ± 0.019	3.477 ± 0.015	3.459 ± 0.045	1.004

Table 2. Details of the fits selected for the final analysis (indicated by a "*" in **Table 1**). Note that the significance of the fitted signal amplitudes (relative to the background) A range from $A/\sigma_A = 2.1$ to 9.8.

Observable	z	Relative amplitude A	Half-width Δ
$\hat{d}_\alpha$	0.56	0.00290 ± 0.00100	0.00169 ± 0.00022
$\hat{d}_/$	0.56	0.00422 ± 0.00069	0.00164 ± 0.00020
$\hat{d}_z$	0.56	0.00505 ± 0.00226	0.00250 ± 0.00041
$\hat{d}_\alpha$	0.34	0.00632 ± 0.00064	0.00225 ± 0.00008
$\hat{d}_/$	0.34	0.00269 ± 0.00044	0.00197 ± 0.00013
$\hat{d}_z$	0.34	0.00341 ± 0.00162	0.00238 ± 0.00035

Table 3. Calculated d_{drag}, $\hat{d}_\alpha$, $\hat{d}_/$, and $\hat{d}_z$ for $z = 0.56$ and $z = 0.34$, as a function of Ω_m, for $\Omega_k = 0$ and $\Omega_{\text{de}}(a) \equiv \Omega_\Lambda$ constant. d_{drag} is the BAO galaxy comoving standard ruler length in units of c/H_0. It is calculated from $d_{\text{drag}} = 1.0184 d_*$, $d_* \equiv \theta_* \chi(z_*)$, $\theta_* = 0.0104092$, $\chi(z_*) \equiv \int_0^{z_*} \mathrm{d}z/E(z)$, $E(a) = \left(\Omega_m/a^3 + \Omega_r/a^4 + \Omega_\Lambda + \Omega_k/a^2\right)^{1/2}$, and $a = 1/(1+z)$. $\hat{d}_\alpha$, $\hat{d}_/$, and $\hat{d}_z$ are calculated with Equations (5), (6), and (7) of [1] with $z_c = 3.79$. The dependence on $h = 0.7$ or $\sum m_\nu = 0.27$ eV is negligible compared to the uncertainties in **Table 5**.

Ω_m	$100 d_{\text{drag}}$	$100\hat{d}_\alpha$	$100\hat{d}_/$	$100\hat{d}_z$	$100\hat{d}_\alpha$	$100\hat{d}_/$	$100\hat{d}_z$
			$z = 0.56$			$z = 0.34$	
0.25	3.628	3.535	3.510	3.477	3.560	3.538	3.510
0.27	3.519	3.457	3.444	3.427	3.471	3.457	3.440
0.28	3.468	3.421	3.414	3.405	3.429	3.420	3.408
0.29	3.420	3.386	3.385	3.384	3.390	3.385	3.377
0.31	3.330	3.323	3.333	3.346	3.317	3.319	3.321
0.33	3.248	3.265	3.285	3.311	3.251	3.259	3.271

The peculiar motion corrections were studied with the galaxy generator described in [5] [9]. Results of these simulations are shown in **Table 4**, for G-G distances, for two cases: "correct $P(k)$" and "correct $P_{\text{gal}}(k)$". The "correct $P(k)$" simulations have the predicted linear power spectrum of density fluctuations $P(k)$ of the ΛCDM model (Equation (8.1.42) of [10]), while the "correct $P_{\text{gal}}(k)$" simulations have a steeper $P(k)$ input so that the generated galaxy power spectrum $P_{\text{gal}}(k)$ matches observations, see Figure 15 of [5]. (The need for the steeper $P(k)$ is currently not understood.) All of these G-G corrections, and also the corrections for LG-LG and G-C, are in agreement, to within a factor 2, with the corrections applied in [1] that where taken from a study in [11]. In summary, in the present analysis we apply the same peculiar motion corrections as in [1], *i.e.* we multiply the measured BAO distances $\hat{d}_\alpha$, $\hat{d}_/$, and $\hat{d}_z$, by correction factors f_α, $f_/$, and f_z, respectively, where

Table 4. Study of peculiar motion corrections to be added to the G-G measurements of $\hat{d}_\alpha$, $\hat{d}_/$, and $\hat{d}_z$ in **Table 1**, obtained from simulations.

z	Simulation	$\Delta\hat{d}_\alpha$	$\Delta\hat{d}_/$	$\Delta\hat{d}_z$
0.5	correct $P(k)$	0.000062	0.000080	0.000112
0.5	correct $P_{\text{gal}}(k)$	0.000096	0.000125	0.000175
0.3	correct $P(k)$	0.000063	0.000080	0.000111
0.3	correct $P_{\text{gal}}(k)$	0.000084	0.000107	0.000148

$$
\begin{aligned}
f_\alpha - 1 &= 0.00320 \cdot a^{1.35}, \\
f_/ - 1 &= 0.00350 \cdot a^{1.35}, \\
f_z - 1 &= 0.00381 \cdot a^{1.35}.
\end{aligned}
\tag{1}
$$

We take half of these corrections as a systematic uncertainty. The effect of these corrections is relatively small as shown in **Table 6**.

Uncertainties of $\hat{d}_\alpha$, $\hat{d}_/$, and $\hat{d}_z$ are presented in **Table 5**. These uncertainties are dominated by cosmological and statistical fluctuations, and are estimated from the root-mean-square fluctuations of many measurements, from the width of the distribution of *Q*, and from the issues discussed in the **Appendix**.

Fits to the two independent selected triplets $\hat{d}_\alpha$, $\hat{d}_/$, and $\hat{d}_z$ indicated by a "*" in **Table 1**, with the uncertainties in **Table 5**, are presented in **Table 6**.

Four Scenarios are considered. In Scenario 1 the dark energy density is constant, *i.e.* $\Omega_{\text{de}}(a) = \Omega_\Lambda$. In Scenario 2 the observed acceleration of the expansion of the universe is due to a gas of negative pressure with an equation of state $w \equiv p/\rho < 0$. We allow the index w to be a function of a [12] [13]: $w(a) = w_0 + w_a(1-a)$. Scenario 3 is the same as Scenario 2, except that w is constant, *i.e.* $w_a = 0$. In Scenario 4 we assume $\Omega_{\text{de}}(a) = \Omega_{\text{de}}\left[1 + w_1(1-a)\right]$.

Note in **Table 6** that Ω_k is consistent with zero, and $\Omega_{\text{de}}(a)$ is consistent with being independent of the expansion parameter *a*. For $\Omega_k = 0$ and $\Omega_{\text{de}}(a) \equiv \Omega_\Lambda$ constant we obtain from **Table 6**:

$$
\Omega_m = 0.288 \pm 0.037, \tag{2}
$$

with $\chi^2 = 1.0$ for 4 degrees of freedom.

Final calculations are done with fits and numerical integrations. Never-the-less, it is convenient to present approximate analytical expressions obtained from the numerical integrations for the case of flat space and a cosmological constant. At decoupling, $z_* = 1089.92 \pm 0.25$ from the Planck "TT, TE, EE + lowE + lensing" measurement [3]. The "angular distance" at decoupling is $D_A(z_*) \equiv \chi(z_*) a_* c/H_0$, with

$$
\chi(z_*) = 3.2675 \left(\frac{h + 0.35 \sum m_\nu}{0.7} \right)^{0.01} \left(\frac{0.28}{\Omega_m} \right)^{0.4}, \tag{3}
$$

which has negligible dependence on h or $\sum m_\nu$.

Table 5. Uncertainties of $\hat{d}_\alpha$, $\hat{d}_/$, and $\hat{d}_z$ at 68% confidence. For "*et al.*" see the **Appendix**.

	$\hat{d}_\alpha$	$\hat{d}_/$	$\hat{d}_z$
Method	±0.00003	±0.00004	±0.00008
Peculiar motion correction	±0.00004	±0.00004	±0.00005
Cosmological *et al.* +			
statistical fluctuations	±0.00029	±0.00055	±0.00070
Total	±0.00030	±0.00055	±0.00071

Table 6. Cosmological parameters obtained from the 6 independent galaxy BAO measurements indicated with a "*" in **Table 1** in several scenarios. Corrections for peculiar motions are given by Equation (1) except, for comparison, the fit "1*" which has no correction. Scenario 1 has $\Omega_{\mathrm{de}}(a)$ constant. Scenario 3 has $w = w_0$. Scenario 4 has $\Omega_{\mathrm{de}}(a) = \Omega_{\mathrm{de}}\left[1 + w_1(1-a)\right]$.

	Scenario 1*	Scenario 1	Scenario 1	Scenario 3	Scenario 4	Scenario 4
Ω_k	0 fixed	0 fixed	0.267 ± 0.362	0 fixed	0 fixed	0.262 ± 0.383
$\Omega_{\mathrm{de}} + 0.6\Omega_k$	0.712 ± 0.037	0.712 ± 0.037	0.738 ± 0.050	0.800 ± 0.364	0.760 ± 0.151	0.745 ± 0.148
w_0	n.a.	n.a.	n.a.	-0.76 ± 0.65	n.a.	n.a.
w_1	n.a.	n.a.	n.a.	n.a.	0.71 ± 2.00	0.13 ± 2.77
$100 d_{\mathrm{drag}}$	3.48 ± 0.06	3.487 ± 0.052	3.48 ± 0.06	3.43 ± 0.16	3.42 ± 0.19	3.48 ± 0.21
χ^2/d.f.	0.9/4	1.0/4	0.4/3	0.9/3	0.9/3	0.4/2

From the Planck "TT, TE, EE + lowE + lensing" measurement [3], $\theta_* = 0.0104092 \pm 0.0000031$. Then the comoving sound horizon at decoupling is $r_* \equiv d_* c / H_0$, with

$$d_* = \theta_* \chi(z_*) = 0.03401 \left(\frac{0.28}{\Omega_m} \right)^{0.4}. \tag{4}$$

The BAO standard ruler for galaxies r_{drag} is larger than r_* because last scattering of electrons occurs after last scattering of photons due to their different number densities. In the present analysis, we take $r_{\mathrm{drag}} \equiv d_{\mathrm{drag}} c / H_0$ with

$$\frac{d_{\mathrm{drag}}}{d_*} = 1.0184 \pm 0.0004, \tag{5}$$

from the Planck "TT, TE, EE + lowE + lensing" analysis, with the uncertainty from Equation (10) of Reference [3]. Note from (4) and Equation (10) of Reference [3] that (5) is insensitive to cosmological parameters, so the uncalibrated analysis decouples from h or $\sum m_\nu$.

We can test (5) experimentally. From **Table 6** we obtain $d_{\mathrm{drag}} = 0.03487 \pm 0.00052$. From (4) and (2) we obtain $d_* = 0.03363 \pm 0.00174$, so the measured $d_{\mathrm{drag}} / d_* = 1.037 \pm 0.056$.

To the 6 independent galaxy BAO measurements, we add the sound horizon angle θ_*, and obtain the results presented in **Table 7**. Note that measurements

Table 7. Cosmological parameters obtained from the 6 independent galaxy BAO measurements indicated with a "*" in **Table 1**, plus θ_* from the Planck experiment, in several scenarios. Corrections for peculiar motions are given by Equation (1). $d_{\text{drag}}/d_* = 1.0184 \pm 0.0004$. Scenario 1 has $\Omega_{\text{de}}(a)$ constant. Scenario 2 has $w(a) = w_0 + w_a(1-a)$. Scenario 3 has $w = w_0$. Scenario 4 has $\Omega_{\text{de}}(a) = \Omega_{\text{de}}[1 + w_1(1-a)]$.

	Scenario 1	Scenario 1	Scenario 2	Scenario 3	Scenario 4	Scenario 4
Ω_k	0 fixed	0.008 ± 0.018	0 fixed	0 fixed	0 fixed	-0.007 ± 0.101
$\Omega_{\text{de}} + 2.1\Omega_k$	0.7276 ± 0.0047	0.724 ± 0.009	0.708 ± 0.080	0.724 ± 0.008	0.723 ± 0.011	0.723 ± 0.011
w_0	n.a.	n.a.	-0.77 ± 1.47	-0.95 ± 0.10	n.a.	n.a.
w_a or w_1	n.a.	n.a.	-0.91 ± 4.53	n.a.	0.19 ± 0.41	0.35 ± 2.20
$100d_*$	3.443 ± 0.024	3.42 ± 0.06	3.35 ± 0.04	3.41 ± 0.07	3.41 ± 0.09	3.39 ± 0.20
χ^2/d.f.	1.2/5	1.0/4	0.9/3	1.0/4	1.0/4	1.0/3

are consistent with flat space and a cosmological constant. Note also that the constraint on Ω_k becomes tighter if $\Omega_{\text{de}}(a)$ is assumed constant, and that the constraint on $\Omega_{\text{de}}(a)$ becomes tighter if Ω_k is assumed zero. In the scenario of flat space and a cosmological constant we obtain

$$\Omega_m = 0.2724 \pm 0.0047, \tag{6}$$

with $\chi^2 = 1.2$ for 5 degrees of freedom. This is the final result of the present analysis.

Adding two measurements in the quasar Lyman-alpha forest [1] [14] [15] we obtain the results presented in **Table 8**. In particular, for flat space and a cosmological constant we obtain

$$\Omega_m = 0.2714 \pm 0.0047, \tag{7}$$

with $\chi^2 = 10.0$ for 7 degrees of freedom. Note that the Lyman-alpha measurements tighten the constraints on Ω_k, w_0, w_1, and w_a.

As a cross-check of the z dependence, from the 4 independent fits to $\hat{d}_\alpha$ at different redshifts z presented in **Figure 3**, plus θ_*, we obtain

$$\Omega_m = 0.2745 \pm 0.0040, \tag{8}$$

with $\chi^2 = 3.0$ for 3 degrees of freedom, for flat space and a cosmological constant.

As a cross-check of isotropy, from the 3 independent fits to $\hat{d}_\alpha$ at $z = 0.36$ shown in **Figure 4** corresponding to different regions of the sky, we obtain

$$\Omega_m = 0.2737 \pm 0.0043, \tag{9}$$

with $\chi^2 = 1.1$ for 2 degrees of freedom, for flat space and a cosmological constant.

To check the stability of $\hat{d}_\alpha$, $\hat{d}_/$, and $\hat{d}_z$ with the data set and galaxy selections, we compare fits highlighted with "*" and "&" in **Table 1**, and also fits in **Figure 5**.

Additional studies are presented in the **Appendix**.

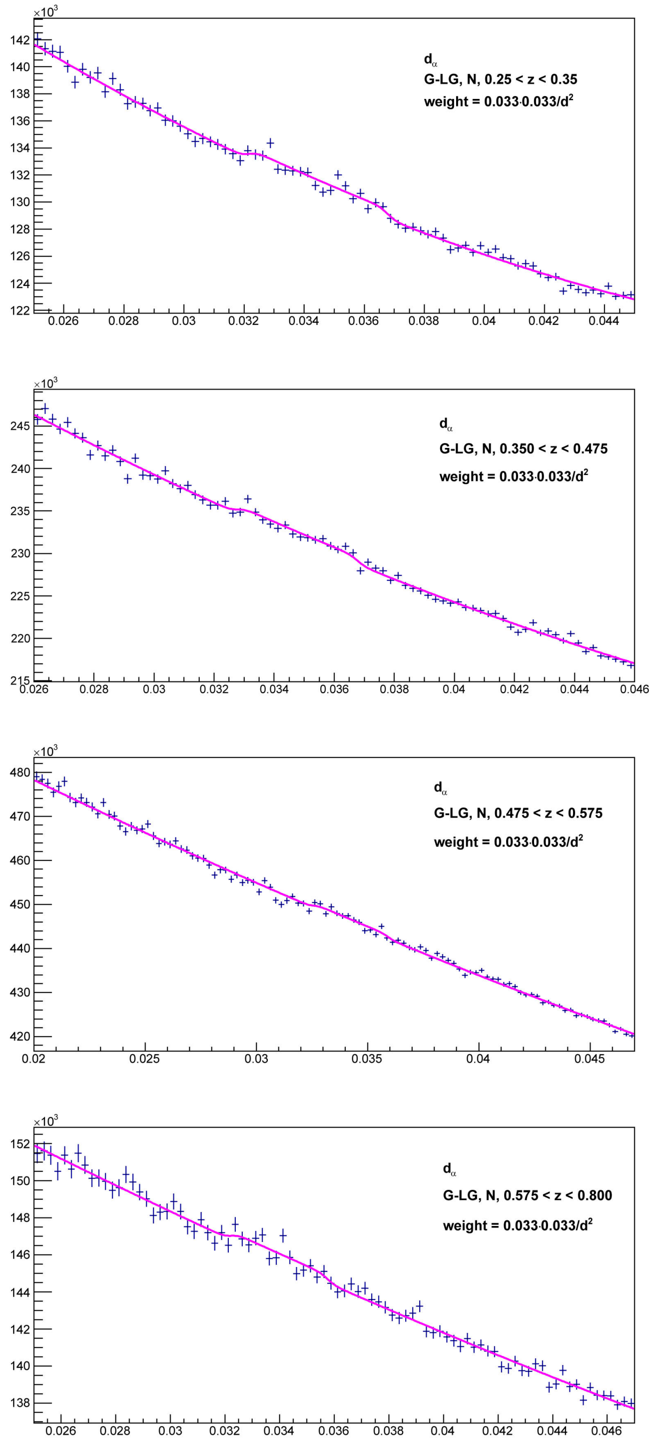

Figure 3. Fits to histograms of G-LG distances d that obtain $\hat{d}_\alpha$ at $z = 0.32, 0.42, 0.53$, and 0.65. The bins of z are $(0.25, 0.35)$, $(0.35, 0.475)$, $(0.475, 0.575)$, and $(0.575, 0.800)$, respectively. The fits obtain $\hat{d}_\alpha = 0.03447 \pm 0.00012$, 0.03478 ± 0.00012, 0.03424 ± 0.00015, and 0.03399 ± 0.00020 respectively, where uncertainties are statistical from the fits. A fit with these four measurements (with the total uncertainties of Table 5), plus θ_* from the Planck experiment, obtains $\Omega_m = 0.2745 \pm 0.0040$ and $d_* = 0.03433 \pm 0.00020$ with $\chi^2 = 3.0$ for 3 degrees of freedom.

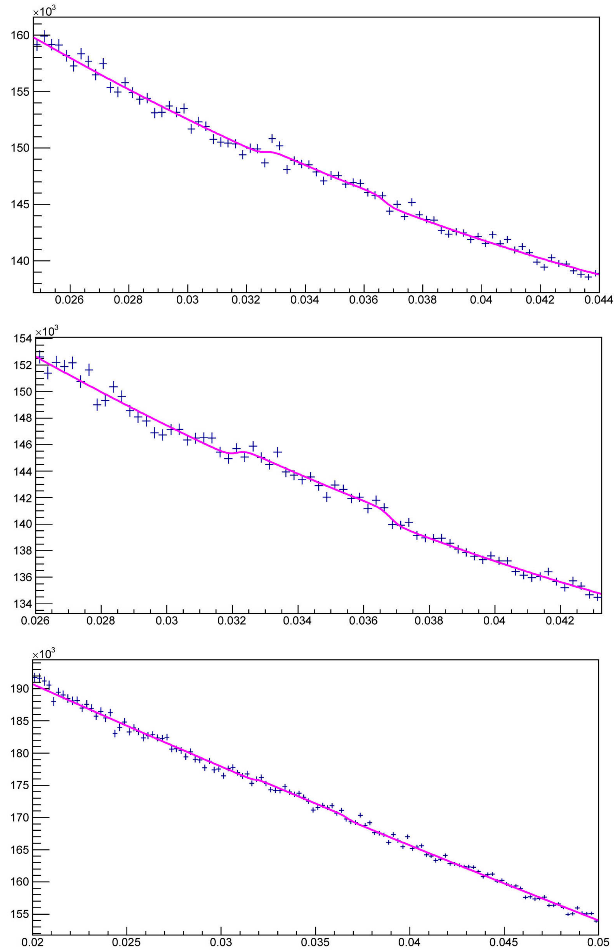

Figure 4. Fits to histograms of G-LG distances d, with z in the range 0.25 - 0.45, that obtain $\hat{d}_\alpha$ at $z = 0.36$. From top to bottom, they correspond to the northern galactic cap with right ascension < 180˚ (NW), to the northern galactic cap with right ascension > 180˚ (NE), and to the southern galactic cap (S). The fits obtain $\hat{d}_\alpha = 0.03468 \pm 0.00012$, 0.03447 ± 0.00012, and 0.03424 ± 0.00019 respectively, where uncertainties are statistical from the fits. A fit with these three measurements (with the total uncertainties of Table 5), plus θ_* from the Planck experiment, obtains $\Omega_m = 0.2737 \pm 0.0043$ and $d_* = 0.03437 \pm 0.00022$ with $\chi^2 = 1.1$ for 2 degrees of freedom.

Table 8. Cosmological parameters obtained from the 6 galaxy BAO measurements indicated with a "*" in Table 1, plus θ_* from the Planck experiment, plus two Lyman-alpha measurements [1] [14] [15] in several scenarios. Corrections for peculiar motions are given by Equation (1). $d_{\text{drag}}/d_* = 1.0184 \pm 0.0004$. Scenario 1 has $\Omega_{\text{de}}(a)$ constant. Scenario 2 has $w(a) = w_0 + w_a(1-a)$. Scenario 3 has $w = w_0$. Scenario 4 has $\Omega_{\text{de}}(a) = \Omega_{\text{de}}\left[1 + w_1(1-a)\right]$.

	Scenario 1	Scenario 1	Scenario 2	Scenario 3	Scenario 4	Scenario 4
Ω_k	0 fixed	-0.011 ± 0.008	0 fixed	0 fixed	0 fixed	-0.022 ± 0.010
$\Omega_{\text{de}} + 2.1\Omega_k$	0.7286 ± 0.0047	0.734 ± 0.006	0.703 ± 0.028	0.726 ± 0.008	0.723 ± 0.011	0.720 ± 0.011
w_0	n.a.	n.a.	-0.70 ± 0.33	-0.96 ± 0.09	n.a.	n.a.
w_a or w_1	n.a.	n.a.	-1.18 ± 1.37	n.a.	0.24 ± 0.40	0.80 ± 0.49
$100d_*$	3.449 ± 0.024	3.48 ± 0.04	3.32 ± 0.13	3.42 ± 0.07	3.40 ± 0.08	3.34 ± 0.09
χ^2/d.f.	10.0/7	7.7/6	8.0/5	9.2/6	9.0/6	4.6/5

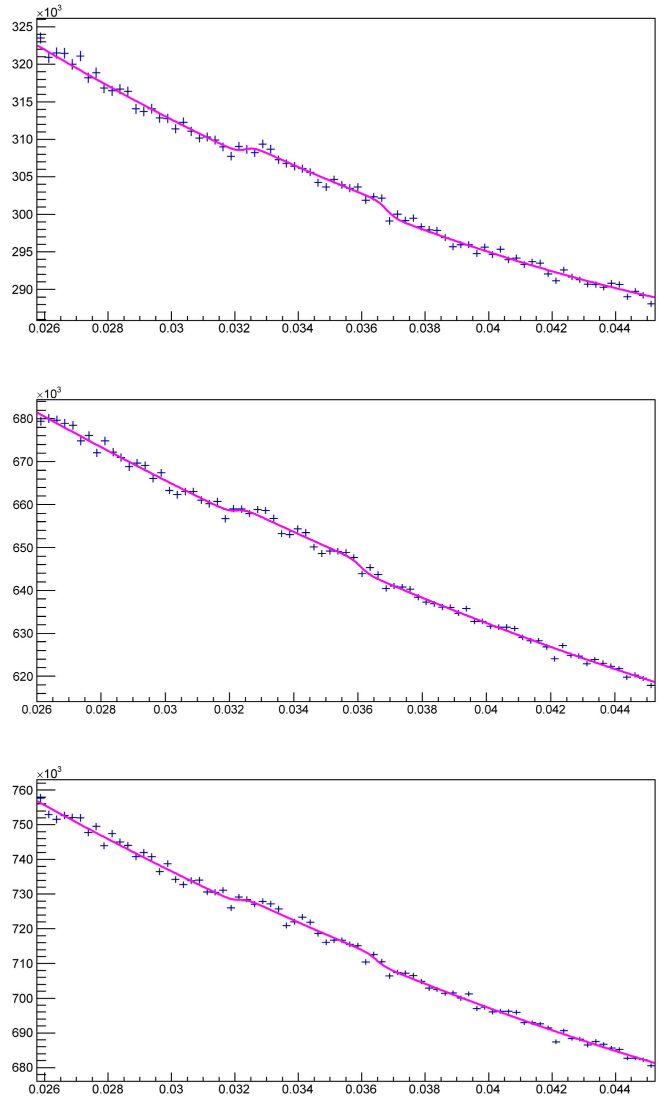

Figure 5. Fits to histograms of G-LG distances d, with z in the range 0.25 - 0.45 for the northern galactic cap (N), that obtain $\hat{d}_\alpha$ at $z = 0.36$. From top to bottom, they correspond to SDSS DR14 (this analysis), DR14 with galaxy selections of [1], and DR13 with galaxy selections of [1]. The fits obtain $\hat{d}_\alpha = 0.03455 \pm 0.00010$, 0.03416 ± 0.00010, and 0.03431 ± 0.00012 respectively, where uncertainties are statistical from the fits. Note that our assigned total uncertainty for $\hat{d}_\alpha$ is ±0.00030. This single fit for the current analysis, together with θ_* obtains $\Omega_m = 0.272 \pm 0.007$ and $d_* = 0.0345 \pm 0.0004$, with zero degrees of freedom. The relative amplitudes A of the fitted signals are 0.00552 ± 0.00060, 0.00369 ± 0.00042, and 0.00341 ± 0.00039 respectively. The number of galaxies (G) and large galaxies (LG) are $(114597, 65130)$, $(153783, 101504)$, and $(160943, 107971)$, respectively. Note that the relative amplitude is larger for the current galaxy selections.

3. Measurement of H_0 with BAO as a *Calibrated* Standard Ruler

We consider the scenario of flat space and a cosmological constant. It is useful to present approximate analytic expressions, tho all final calculations are done directly with fits to the measurements marked with a "*" in **Table 1** and numerical integrations to obtain correct uncertainties for correlated parameters.

To calibrate the BAO measurements, we integrate the comoving photon-electron-baryon plasma sound speed from $t=0$ up to decoupling and obtain the "comoving acoustic horizon distance" $r_* \equiv d_* c/H_0$, with

$$d_* = 0.03407\left(\frac{h+0.026\sum m_\nu}{0.7}\right)^{0.513}\left(\frac{0.28}{\Omega_m}\right)^{0.244}\left(\frac{0.0225}{\Omega_b h^2}\right)^{0.097}. \tag{10}$$

The acoustic angular scale is

$$\theta_* \equiv \frac{d_*}{\chi(z_*)} = 0.010427\left(\frac{h+0.020\sum m_\nu}{0.70}\right)^{0.503}\left(\frac{\Omega_m}{0.28}\right)^{0.156}\left(\frac{0.0225}{\Omega_b h^2}\right)^{0.097}, \tag{11}$$

in agreement with Equation (11) of [3].

Let us now consider the measurement of h. From the galaxy BAO measurements in **Table 6** we obtain $\Omega_m = 0.288 \pm 0.037$ and $d_{\text{drag}} = 0.03487 \pm 0.00052$. From Big Bang Nucleosynthesis, $\Omega_b h^2 = 0.0225 \pm 0.0008$ at 68% confidence [4]. From this data and Equations (5) and (10), or the corresponding fit, we obtain

$$h + 0.026\sum m_\nu = 0.716 \pm 0.027, \tag{12}$$

with $\chi^2 = 1.0$ for 4 degrees of freedom.

The Planck measurement of θ_* allows a more precise measurement of h. From **Table 7**, we obtain $\Omega_m = 0.2724 \pm 0.0047$. Then from Big Bang Nucleosynthesis and (11), or the corresponding fit, we obtain

$$h + 0.020\sum m_\nu = 0.7038 \pm 0.0060, \tag{13}$$

with $\chi^2 = 1.2$ for 5 degrees of freedom. Note that the uncertainties of h and Ω_m are correlated through Equation (11).

4. Studies of CMB Fluctuations

In **Table 9**, we present a qualitative study of the sensitivity of the CMB power spectrum $l(l+1)C^S_{TT,l}/(2\pi)$ to constrain Ω_m and $\sum m_\nu$. We use the approximate analytic expression (7.2.41) of [10], modified to include $\sum m_\nu$, to compare the spectra with Planck 2018 "TT, TE, EE + lowE + lensing" parameters with the best fit spectra with fixed values $\Omega_m = 0.2854$ and $\sum m_\nu = 0.06, 0.1, 0.2, 0.3, 0.4, 0.5$ eV. We find that the differences in spectra range from 0.11% to 0.3% of the first acoustic peak, see **Figure 6**. So the CMB power spectrum, while being very sensitive to constrain θ_*, has low sensitivity to constrain Ω_m or $\sum m_\nu$.

In view of the low sensitivity of the CMB power spectra to constrain Ω_m, the Planck analysis can benefit from a combination with the direct measurement of Ω_m given by Equation (6). The combination, obtained with the "base_mnu_plikHM_TTTEEE_lowTEB_lensing_*.txt MC chains" made public by the Planck Collaboration [3], is presented in **Table 10**. This combination is preliminary due to the sparseness of the MC chains at low values of Ω_m.

Table 9. Cosmologies with fixed Ω_m and $\sum m_\nu$ fitted to the CMB power spectrum $l(l+1)C^S_{TT,l}/(2\pi)$ with the Planck 2018 "TT, TE, EE + lowE + lensing" parameters $\Omega_m = 0.3153$, $\sum m_\nu = 0.06$ eV, $h = 0.6736$, $\Omega_b h^2 = 0.02237$, $n_s = 0.9649$, $N^2 = 1.670 \times 10^{-10}$, and $\tau = 0.0544$ [3]. The approximate analytic Equation (7.2.41) of [10] (modified to include $\sum m_\nu$) was used. Notation: $N^2 \equiv A_s/(4\pi) \equiv \Delta_R^2/(4\pi)$.

Ω_m	0.2854	0.2854	0.2854	0.2854	0.2854	0.2854
$\sum m_\nu$ [eV]	0.06	0.1	0.2	0.3	0.4	0.5
h	0.6980	0.6976	0.6965	0.6954	0.6942	0.6931
$100\Omega_b h^2$	2.282	2.288	2.306	2.324	2.343	2.362
n_s	0.9692	0.9699	0.9716	0.9735	0.9754	0.9774
$10^{10} N^2$	1.730	1.729	1.725	1.722	1.716	1.713
τ	0.0774	0.0778	0.0787	0.0797	0.0799	0.0809
r.m.s. [μK^2]	6.07	6.98	9.29	11.66	14.06	16.49

Table 10. Combination of the Planck 2018 "TT, TE, EE + lowE + lensing" analysis [3] with the directly measured $\Omega_m = 0.2724 \pm 0.0047$. Uncertainties are at 68% confidence. The Planck $\chi_P^2 \equiv -2 \cdot \ln \mathcal{L}$ increases from 12,956.78 to 12,968.64 with this combination. The galaxy $\chi_G^2 \equiv (\Omega_m - 0.2724)^2 / 0.0047^2$. Preliminary.

	Planck	Planck + Ω_m
$\Omega_b h^2$	0.02237 ± 0.00015	0.02265 ± 0.00012
$\Omega_c h^2$	0.1200 ± 0.0012	0.1155 ± 0.0005
$100\theta_*$	1.04092 ± 0.00031	1.04125 ± 0.00022
τ	0.0544 ± 0.0073	0.078 ± 0.006
$\ln 10^{10} A_s$	3.044 ± 0.014	3.102 ± 0.020
n_s	0.9649 ± 0.0042	0.9726 ± 0.0017
Ω_Λ	0.6847 ± 0.0073	0.7147 ± 0.0040
Ω_m	0.3153 ± 0.0073	0.2853 ± 0.0040
h	0.6736 ± 0.0054	0.6990 ± 0.0030
σ_8	0.8111 ± 0.0060	0.8346 ± 0.0054
χ^2_P	12,956.78	12,968.64
χ^2_G	83.31	7.53
χ^2_{tot}	13,040.09	12,976.17

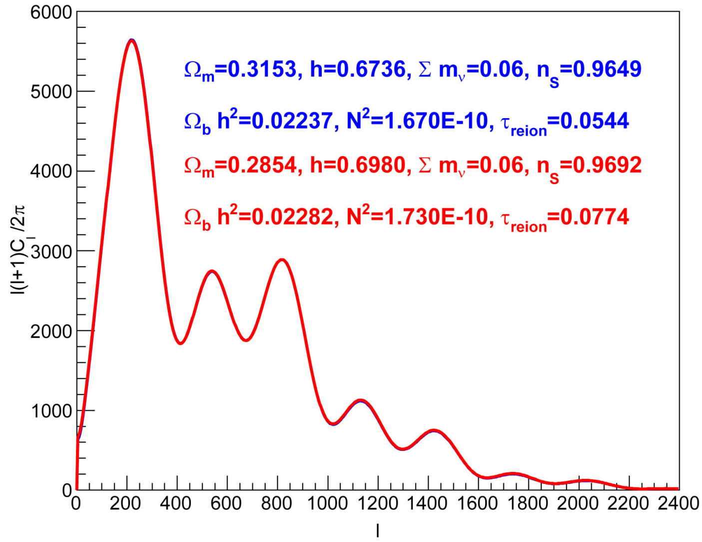

Figure 6. Comparison of the power spectra $l(l+1)C^S_{TT,l}/(2\pi)$ [μK^2] for the Planck 2018 "TT, TE, EE + lowE + lensing" parameters, with the best fit spectra with $\Omega_m = 0.2854$ and $\sum m_\nu = 0.06$ eV fixed, calculated with the approximate Equation (7.2.41) of [10] (modified to include $\sum m_\nu$). The r.m.s. difference is 6.07 μK^2, corresponding to 0.11% of the first acoustic peak, so the two spectra can not be distinguished by eye.

5. Tensions

We consider four direct measurements: 1) $h = 0.7348 \pm 0.0166$ by the Sh$_0$es Team [16], 2) $\sigma_8 \approx [0.746 \pm 0.012(stat) \pm 0.022(syst)](0.3/\Omega_m)^{0.47}$ from the abundance of rich galaxy clusters [4] [17], 3) $\sigma_8 \approx [0.745 \pm 0.039](0.3/\Omega_m)^{0.5}$ from weak gravitational lensing [4] [18], and 4) $\Omega_m = 0.2724 \pm 0.0047$ from galaxy BAO and θ_* from Planck, Equation (6) of this analysis. Comparing these measurements with Planck (left hand column of **Table 10**) we obtain differences of 3.5σ, 2.5σ, 1.8σ, and 4.9σ, respectively. Comparing these measurements with the Planck + Ω_m combination (right hand column of **Table 10**) we obtain differences of 2.1σ, 2.3σ, 1.5σ, and 2.1σ, respectively. In conclusion, the Planck + Ω_m combination reduces the tensions with the direct measurements. Note that the Planck + Ω_m combination has σ_8 greater than the direct measurements. This 2.7σ tension may be due to neutrino masses.

6. Update on Neutrino Masses

We consider the scenario of three neutrino flavors with eigenstates of nearly the same mass, so $\sum m_\nu \approx 3m_\nu$. Massive neutrinos suppress the power spectrum of linear density fluctuations $P(k)$ by a factor $1 - 8\Omega_\nu/\Omega_m$ for $k \gg 0.018 \cdot \Omega_m^{1/2} \left(\sum m_\nu / 1\,\text{eV}\right)^{1/2} h$ Mpc^{-1} [19]. This suppression affects σ_8 and the galaxy power spectrum $P_{gal}(k)$, *but does not* affect the Sachs-Wolfe effect at low k. So, by comparing fluctuations at large and small k it is possible to constrain or measure $\sum m_\nu$ [5].

To obtain $\sum m_\nu$ we minimize a χ^2 with four terms corresponding to N^2,

σ_8, and two parameters obtained from the Planck + Ω_m combination: $h = 0.6990 \pm 0.0030$, and $n_s = 0.9726 \pm 0.0017$. In the fit, Ω_m is obtained from Equation (11), and $\Omega_b h^2 = 0.02265 \pm 0.00012$. σ_8 is obtained from the combination of the two direct measurements presented in Section 5.

For $N^2 = (2.08 \pm 0.33) \times 10^{-10}$ [5] obtained from the Sachs-Wolfe effect measured by the COBE satellite (see list of references in [10]) we obtain

$$\sum m_\nu = 0.45 \pm 0.20 \text{ eV}, \tag{14}$$

with zero degrees of freedom, in agreement with [5] where the method is explained in detail.

Since $\sum m_\nu < 1.7$ eV, neutrinos are still ultra-relativistic at decoupling. Then there is no power suppression of the CMB fluctuations, and we can use the entire spectrum to fix the amplitude N^2. From the Planck + Ω_m combination of **Table 10** we obtain $N^2 \equiv A_s/(4\pi) = (1.7700 \pm 0.0354) \times 10^{-10}$, and

$$\sum m_\nu = 0.26 \pm 0.08 \text{ eV}, \tag{15}$$

with zero degrees of freedom.

To strengthen the constraints from the two direct measurements of σ_8, we add to the fit measurements of fluctuations of number counts of galaxies in spheres of radii $16/h$, $32/h$, $64/h$, and $128/h$ Mpc, as explained in [5]. We obtain

$$\sum m_\nu = 0.27 \pm 0.08 \text{ eV}, \tag{16}$$

with $\chi^2 = 1.6$ for 2 degrees of freedom, and find no significant pulls on N^2, h, or n_s. These results are sensitive to the accuracy of the direct measurements of σ_8.

Acknowledgements

We have used data in the publicly released Sloan Digital Sky Survey SDSS DR14 catalog.

Funding for the Sloan Digital Sky Survey (SDSS) has been provided by the Alfred P. Sloan Foundation, the Participating Institutions, the National Aeronautics and Space Administration, the National Science Foundation, the US Department of Energy, the Japanese Monbukagakusho, and the Max Planck Society. The SDSS Web site is http://www.sdss.org/.

The SDSS is managed by the Astrophysical Research Consortium (ARC) for the Participating Institutions. The Participating Institutions are The University of Chicago, Fermilab, the Institute for Advanced Study, the Japan Participation Group, The Johns Hopkins University, Los Alamos National Laboratory, the Max-Planck-Institute for Astronomy (MPIA), the Max-Planck-Institute for Astrophysics (MPA), New Mexico State University, University of Pittsburgh, Princeton University, the United States Naval Observatory, and the University of Washington.

We have also used data publicly released by the Planck Collaboration [3] in the form of "MC chains", and the corresponding analysis tool "GetDist GUI".

Conflicts of Interest

The author declares no conflicts of interest regarding the publication of this paper.

References

[1] Hoeneisen, B. (2017) Study of Baryon Acoustic Oscillations with SDSS DR13 Data and Measurements of Ω_k and $\Omega_{de}(a)$. *International Journal of Astronomy and Astrophysics*, **7**, 11-27. https://doi.org/10.4236/ijaa.2017.71002

[2] Patrignani, C., *et al.* (Particle Data Group) (2016) Review of Particle Physics. *Chinese Physics C*, **40**, 100001. https://doi.org/10.1088/1674-1137/40/10/100001

[3] Aghanim, N., *et al.* (2018) Planck 2018 Results. VI. Cosmological Parameters, arXiv:1807.06209.

[4] Tanabashi, M., *et al.* (Particle Data Group) (2018) The Review of Particle Physics. *Physical Review D*, **98**, 030001.

[5] Hoeneisen, B. (2018) Study of Galaxy Distributions with SDSS DR14 Data and Measurement of Neutrino Masses. *International Journal of Astronomy and Astrophysics*, **8**, 230-257. https://doi.org/10.4236/ijaa.2018.83017

[6] Blanton, M.R., *et al.* (2017) Sloan Digital Sky Survey IV: Mapping the Milky Way, Nearby Galaxies, and the Distant Universe. *The Astronomical Journal*, **154**, 28, 35.

[7] Dawson, K.S., *et al.* (2013) The Baryon Oscillation Spectroscopic Survey of SDSS-III. *The Astronomical Journal*, **145**, 10, 41.

[8] Eisenstein, D.J., Seo, H.-J. and White, M. (2007) On the Robustness of the Acoustic Scale in the Low-Redshift Clustering of Matter. *ApJ*, **664**, 660-674. https://doi.org/10.1086/518755

[9] Hoeneisen, B. (2000) A Simple Model of the Hierarchical Formation of Galaxies. arXiv:astro-ph/0009071.

[10] (2008) Steven Weinberg, Cosmology. Oxford University Press, Oxford.

[11] Seo, H.-J., *et al.* (2010) High-Precision Predictions for the Acoustic Scale in the Non-Linear Regime. *ApJ*, **720**, 1650. https://doi.org/10.1088/0004-637X/720/2/1650

[12] Chevallier, M. and Polarski, D. (2001) Accelerating Universes with Scaling Dark Matter. *International Journal of Modern Physics*, **D10**, 213. https://doi.org/10.1142/S0218271801000822

[13] Linder, E.V. (2003) Exploring the Expansion History of the Universe. *Physical Review Letters*, **90**, 091301. https://doi.org/10.1103/PhysRevLett.90.091301

[14] Font-Ribera, A., *et al.* (2014) Quasar-Lyman Forest Cross-Correlation from BOSS DR11: Baryon Acoustic Oscillations. *Journal of Cosmology and Astroparticle Physics*, **5**, arXiv:1311.1767. https://doi.org/10.1088/1475-7516/2014/05/027

[15] Delubac, T., *et al.* (2014) Baryon Acoustic Oscillations in the Lyα forest of BOSS DR11 Quasars. arXiv:1404.1801v2.

[16] Riess, A.G., Casertano, S., Yuan, W., *et al.* (2018) New Parallaxes of Galactic Cepheids from Spatially Scanning the Hubble Space Telescope: Implications for the Hubble Constant. *The Astrophysical Journal*, **861**, 126.

[17] Vikhlinin, A., *et al.* (2009) Chandra Cluster Cosmology Project III: Cosmological Parameter Constraints. *The Astrophysical Journal*, **692**, 1060-1074. https://doi.org/10.1088/0004-637X/692/2/1060

[18] Hildebrandt, H., *et al.* (2017) KiDS-450: Cosmological Parameter Constraints from

Tomographic Weak Gravitational Lensing. *Monthly Notices of the Royal Astronomical Society*, **465**, 1454-1498. https://doi.org/10.1093/mnras/stw2805

[19] Lesgourgues, J. and Pastor, S. (2006) Massive Neutrinos and Cosmology. *Physics Reports*, **429**, 307-379. https://doi.org/10.1016/j.physrep.2006.04.001

[20] Eisenstein, D.J. and Hu, W. (1997) Baryonic Features in the Matter Transfer Function.

Appendix

1) Comparison with Reference [1]

Table 4 and Table 5 of Reference [1] can be compared with Table 6 and Table 7 of the present analysis. We find agreement between all measurements when d in Reference [1] is identified with d_* in the present analysis. We find that d in Table 4 of Reference [1] is biased low with respect to d_{drag} in Table 6 of the present analysis. For the scenario of flat space and a cosmological constant, Table 4 of Reference [1] obtains $\Omega_m = 0.284 \pm 0.014$ and $d = 0.0339 \pm 0.0002$. From this Ω_m and Equation (4) we obtain $d_* = 0.0338 \pm 0.0007$, in good agreement with d, so in Reference [1] no correction for d_{drag}/d_* was needed or applied.

2) Bias of BAO measurements of small galaxy samples

We have investigated the difference of d_{drag} between Reference [1] and the present analysis. This difference is not due to the change of data set from SDSS DR13 to SDSS DR14: we have compared the coordinates of selected galaxies and have found no changes in calibrations. The fluctuation is not caused by the tighter galaxy selection requirements of the present analysis: compare the entries with "&" and "*" in Table 1, and see Figure 5.

As an extreme test, we divide the bin $0.425 < z < 0.725$ into 6 sub-samples: $0.425 < z < 0.525$ N, $0.525 < z < 0.625$ N, $0.625 < z < 0.725$ N, $0.425 < z < 0.525$ S, $0.525 < z < 0.625$ S, and $0.625 < z < 0.725$ S. We try to fit each one, and average the successful fits (only about half are successful), and obtain $\hat{d}_\alpha = 0.03358 \pm 0.00015$, $\hat{d}_/ = 0.03415 \pm 0.00027$, and $\hat{d}_z = 0.03335 \pm 0.00033$. We also fit the sum of these six bins, and obtain $\hat{d}_\alpha = 0.03496 \pm 0.00015$, $\hat{d}_/ = 0.03459 \pm 0.00010$, and $\hat{d}_z = 0.03464 \pm 0.00034$. So there is evidence that fits become biased low as the number of galaxies is reduced and the significance of the fitted relative amplitude A of the BAO signal becomes marginal. The reason is that the observed BAO signal has a sharper and larger lower edge at $d \approx 0.032$ compared to the upper edge at ≈0.037, so the upper edge tends to get lost in the background fluctuations as the number of galaxies is reduced.

To reduce this bias, in the present analysis we require the significance of the fitted relative amplitudes $A/\sigma_A > 2$, instead of >1 for Reference [1]. The price to pay is that we obtain only 2 independent bins of z, instead of 6.

3) A study of the BAO signal

The BAO signal has a "step-up-step-down" shape with center at $\hat{d}$ and half-width Δ. The widths of fits vary typically from $\Delta = 0.0017$ to 0.0025, see Table 2. We have used the center $\hat{d}$ as the BAO standard ruler, but could have used the lower edge of the signal at $\hat{d} - \Delta$, or the upper edge at $\hat{d} + \Delta$, or somewhere in between, *i.e.* $\hat{d} + \epsilon\Delta$. We have investigated the value of ϵ that minimizes the root-mean-square fluctuations of a representative selection of measurements. The result is $\epsilon = -0.17$, and the difference in the r.m.s. values is negligible (0.00037 vs. 0.00039) so we keep the center of the signal as our standard ruler, *i.e.* $\epsilon = 0$. The r.m.s. fluctuation of the lower edge with $\epsilon = -1$ is 0.00068, and the fluctuation of the upper edge with $\epsilon = 1$ is 0.00091, which again illustrates the bias described in Appendix 7.2, *i.e.* the lower edge fluctuates less than the upper edge.

A separate open question is whether this center $\hat{d}$ coincides with the d_{drag} of Equation (5)?

Yet another question is this: what value of ϵ would reproduce the Planck Ω_m? We obtain ϵ ranging from −0.81 for $\hat{d}_\alpha$ at $z = 0.34$, to $\epsilon = -0.43$ for $\hat{d}_z$ at $z = 0.56$. These large values of $|\epsilon|$, and their strong dependence on z and galaxy-galaxy orientation, do not seem plausible.

Finally, how well do we understand d_{drag}/d_*? The present study takes $z_{\text{drag}} = 1059.94 \pm 0.30$ and $d_{\text{drag}}/d_* = 1.0184 \pm 0.0004$ from the Planck analysis [3]. Note the extremely small uncertainty obtained by the Planck Collaboration. In comparison, from Equation (4) of Reference [20] we obtain $z_{\text{drag}} = 1020.82$ and $d_{\text{drag}}/d_* = 1.044$.

An estimate of the uncertainties due to the issues discussed in this Appendix is included in **Table 5**.